J. Membrane Biol. 132, 229–241 (1993)

The Journal of
Membrane Biology

A Comparison of K^+ Channel Characteristics in Human T Cells: Perforated-Patch *versus* Whole-Cell Recording Techniques

Dorothy R. Oleson, Louis J. DeFelice, and Robert M. Donahoe
Department of Psychiatry, and Department of Anatomy and Cell Biology, Emory University, Atlanta, Georgia

Summary. Standard whole-cell records using the patch-clamp technique are obtained after rupturing the cell membrane just below the patch pipette. Inherent problems, such as the disruption of cellular architecture and the displacement of cytosol, are unavoidable. In the present report, a whole-cell recording technique which makes use of a monovalent cation ionophore, nystatin, was applied to lymphocytes. Nystatin-perforated patches allow electrical access to the cell interior while virtually blocking the diffusion of cellular constituents into the electrode. By comparing standard whole-cell and perforated-patch techniques we observed marked differences in: activation, inactivation, and deactivation kinetics; steady-state inactivation; and the conductance-voltage relationship of K^+ currents in activated human T cells.

Key Words T lymphocytes · potassium channels · patch clamping · electrophysiology

Introduction

Prolonged depolarization of T cells in the presence of high K^+ solutions can bypass the antigen receptor complex (TCR-CD3) and induce proliferation [31]. In addition, the membrane potential (V_m) appears to play a major role in T cell signal transduction by regulating the influx of Ca^{2+} through ligand-gated channels that open following stimulation of TCR-CD3 [10, 26]. T cells treated with K^+ channel blockers depolarize, indicating that K^+ channels regulate V_m and thereby influence Ca^{2+} influx [17]. Conversely, both intracellular and extracellular Ca^{2+} ion concentrations regulate T cell K^+ channel function by accelerating inactivation and diminishing the number of channels capable of being activated [2, 12]. The intimate connection between cation fluxes across lymphocytic membranes is apparent; however, their relationship following antigenic challenge, and the mechanisms behind the dependence of T cell activity on ionic fluxes, remain largely undiscovered. The perforated-patch technique allows intracellular divalent ions, such as Ca^{2+}, to change without the presence of disrupting nonphysiologic buffers in the intracellular space [14, 18].

The major voltage-gated K^+ channel in T cells is an inactivating delayed rectifier [5, 24, 30], which has been cloned and expressed in *Xenopus* oocytes [9]. It is related to the *Drosophila Shaker* A-channel, and shares 60 to 70% of its amino acids with the Shaker core sequence. The T cell K^+ channel is comprised of 525 amino acids and appears to have six transmembrane domains (S1–S6), which conform to the pattern seen in primary subunits of voltage-gated Na^+ and Ca^{2+} channels [13]. Multimeric subunit assembly or interaction with another protein is likely due to the presence of a leucine zipper [9]. Potential phosphorylation sites are numerous; multiple serine, threonine, and tyrosine residues are present as well as a possible protein kinase A site. Stimulation of the antigen receptor complex (TCR-CD3) activates tyrosine kinases and phosphatases, induces the turnover of phosphotidylinositol 4,5 biphosphate (PIP_2), and increases the production of cyclic adenosine monophosphate (cAMP) [7, 16, 19, 25]. Thus, stimulation of TCR-CD3 may regulate T cell K^+ channels through a variety of potential phosphorylation and/or dephosphorylation events. In this report, we used a permeabilized membrane technique, as first proposed by Lindau and Fernandez [23] and developed by Horn and Marty [14], through which identification of an interface between stimulation of TCR-CD3 and K^+ conductance (gK) in lymphocytes may be facilitated.

Materials and Methods

Cell Preparation

Lymphocyte isolation and culture were designed to obtain activated, essentially pure T cell populations. Human subjects, ages 25–40, were volunteers from the Pheresis Unit of Emory Univer-

sity Hospital. The Pheresis Unit nursing staff informed volunteers of risks associated with leukapheresis and obtained signed acknowledgments from the subjects in accordance with Emory University's Institutional Review Board. Peripheral blood mononuclear cells (PBMC) were isolated by density gradient centrifugation on Ficoll Paque (Pharmacia, Uppsala, Sweden). Separation of T and B lymphocytes from monocytes and remaining platelets was completed by adherence to plastic and a Sepracell gradient (Sepratech, Oklahoma City, OK). Lymphocytes were frozen in Roswell Park Memorial Institute (RPMI) 1640 media (GIBCO, Grand Island, NY) containing 10% dimethyl sulfoxide (Sigma, St. Louis, MO) and 50% fetal bovine serum (FBS) (Hyclone, Logan, UT). Cryopreserved cells, frozen no longer than six months, were rapidly thawed at 37°C, washed, and resuspended in complete medium [RPMI 1640 supplemented with: 10% FBS, 2 mM L-glutamine (GIBCO), and 20 μg/ml gentamycin (Sigma)] at a concentration of 10^6/ml and incubated at 37°C in a 5% CO_2 atmosphere. On the following day, lymphocytes were stimulated with 5 μg/ml phytohemmaglutinin (PHA) (Sigma) and 40 units/ml recombinant human interleukin-2 (rIL-2) (Boehringer Mannheim, Indianapolis, IN). Subsequently, every 72 hr cells were counted and resuspended at a concentration of 2×10^6/ml in fresh complete medium supplemented with 40 units/ml rIL-2. PHA-activated human T cells, isolated from peripheral blood, convert from a mixed population of naive and memory cells to an essentially pure memory cell population within 3–5 days [1, 28, 29]. Using these so-called "primed" T cells reduced variability in gK between cells considerably. All experiments were performed on cells cultured from 5–14 days.

Electrodes and Solutions

Patch electrodes of 3–5 MΩ were pulled from borosilicate glass and fire-polished right before use. Gigaohm seals were routinely achieved by applying negative pressure of approximately 30–40 cm H_2O for 1–2 sec to the pipette and catching the cells directly above the bottom of a 35-mm plastic petri dish; negative pressure was then immediately released. On occasion, additional suction of a smaller magnitude (10–20 cm H_2O) was necessary to seal the cells. Whole-cell currents were recorded following: (A) rupture of the membrane pulled within an electrode filled with (in mM) 125 K-aspartate, 30 KCl, 4 NaCl, 2 $MgCl_2$, 0.55 $CaCl_2$, 1.1 EGTA (pCa 7), and 10 K-HEPES, pH 7.2, 297 mOsm, or alternatively (B) by perforating the membrane patch with nystatin (50–100 μg/ml) in an electrode filled with (in mM) 125 K-aspartate, 30 KCl, 4 NaCl, 1 EGTA, and 10 K-HEPES, pH 7.2, 293 mOsm. Nystatin (Sigma) was dissolved in HPLC grade methanol (Fisher Scientific) at a concentration of 5 mg/ml, sonicated, and stored at 4°C for up to three days. All experiments were done at room temperature (24–27°C). Bath solutions consisted of a standard solution composed of (mM) 140 NaCl, 5 KCl, 2 $CaCl_2$, 2 $MgCl_2$, and 10 Na-HEPES, pH 7.4, 290 mOsm, or a Ca^{2+}-free bath solution composed of (mM) 140 NaCl, 5 KCl, 4 $MgCl_2$, 1 EGTA, and 10 Na-HEPES, pH 7.4, 295 mOsm.

Equipment and Data Analysis

Cells were voltage clamped by controlling the positive input of a current-voltage converter (List L/M EPC-7, List Electric, Darmstadt/Eberestadt, Germany). Membrane voltage was clamped, or held at a specific level, and the currents required to maintain that voltage were recorded with the List L/M EPC-7 low-pass filtered at a bandwidth of 5 kHz (Ithaco 4302 dual filter, Ithaca, NY). Experiments were monitored on a Nicolet 4094C digital oscilloscope (Nicolet, Madison, WI) interfaced with an analog-digital converter (Neuro-corder DR-484, Neuro Data Instruments, NY, NY) and recorded on video tape. A holding potential of $E = -60$ mV was maintained throughout all experiments with the exception of steady-state inactivation. Data analysis was accomplished by employing software programs, FIT and WAVES, developed by William Goolsby and Louis J. DeFelice, Anatomy and Cell Biology Department, Emory University School of Medicine, Atlanta, GA. FIT, a nonlinear curve-fitting program that uses least-squares criterion to determine convergence, was utilized to calculate inactivation time constants. WAVES, an advanced integrative mathematical program, was used to download digitized waveforms from the Nicolet to a personal computer for further analysis (IBM PS/2, Armonk, NY) and to correct for linear leakage. Records were leak subtracted from current responses to voltage steps from $E = -100$ to -50 mV, delivered in 10-mV increments immediately before a series of voltage steps used to determine the *I-V* relationship. When appropriate, data are represented as mean ± SEM.

Formation of Nystatin Pores

Nystatin-containing electrodes form gigaohm seals far less frequently than standard electrodes and do not always achieve an acceptable access resistance [14, 18]. Optimal concentrations ranged from 50–100 μg/ml, formed pores within 10 min, and produced an access resistance of 20–50 MΩ. Precise temporal comparisons between the two techniques are not possible due to time elapsed during pore formation. However, since most alterations in lymphocyte K^+ channel characteristics occur during the first ten minutes of whole-cell recording [3, 8], the time elapsed during construction of nystatin pores would make differences between the two techniques smaller, not greater. In K-aspartate solutions, nystatin pores were stable and T cells remained electrically viable for longer than 30 min. T cells deteriorated rapidly in the presence of 140 mM KCl and the patch spontaneously ruptured with as little as 10 μg/ml of nystatin in KF solutions. Therefore, aspartate was the anion of choice. K-aspartate solutions are second only to KF solutions in their ability to stabilize T cell electrical properties [3], and serve as a basis of comparison between the present report and those of others [3, 12, 22].

Gigaohm seal formation was monitored with a test pulse of 10 mV, duration 10 msec; transient capacitance due to the recording pipette was canceled with the C-FAST circuitry of the List L/M EPC-7 for both whole-cell and perforated-patch recordings. Whole-cell configuration was achieved by applying brief bursts of negative pressure to the cell membrane within the electrode. An abrupt increase in the capacitive transient was used as an indication of electrical access to the cell interior (Fig. 1*A*). Perforated-patch configuration was attained by passively observing a gradual increase in the amplitude and decay of the capacitive current (Fig. 1*B*). The membrane capacitance (C_m) and access (series) resistance (R_a) were estimated by canceling the remaining capacitive transient with the C-SLOW and G-SERIES controls, respectively, of the List amplifier. The series resistance circuitry of the List amplifier (RS-COMP) was not used. C_m values obtained with the perforated-patch method ranged from 2.7–5.2 pF, and agreed closely with whole-cell C_m values ranging from 2.9–6.4 pF. R_a was ~4× higher during perforated-patch recordings, increasing the average time constant ($C_m R_a$) of the capacitive tran-

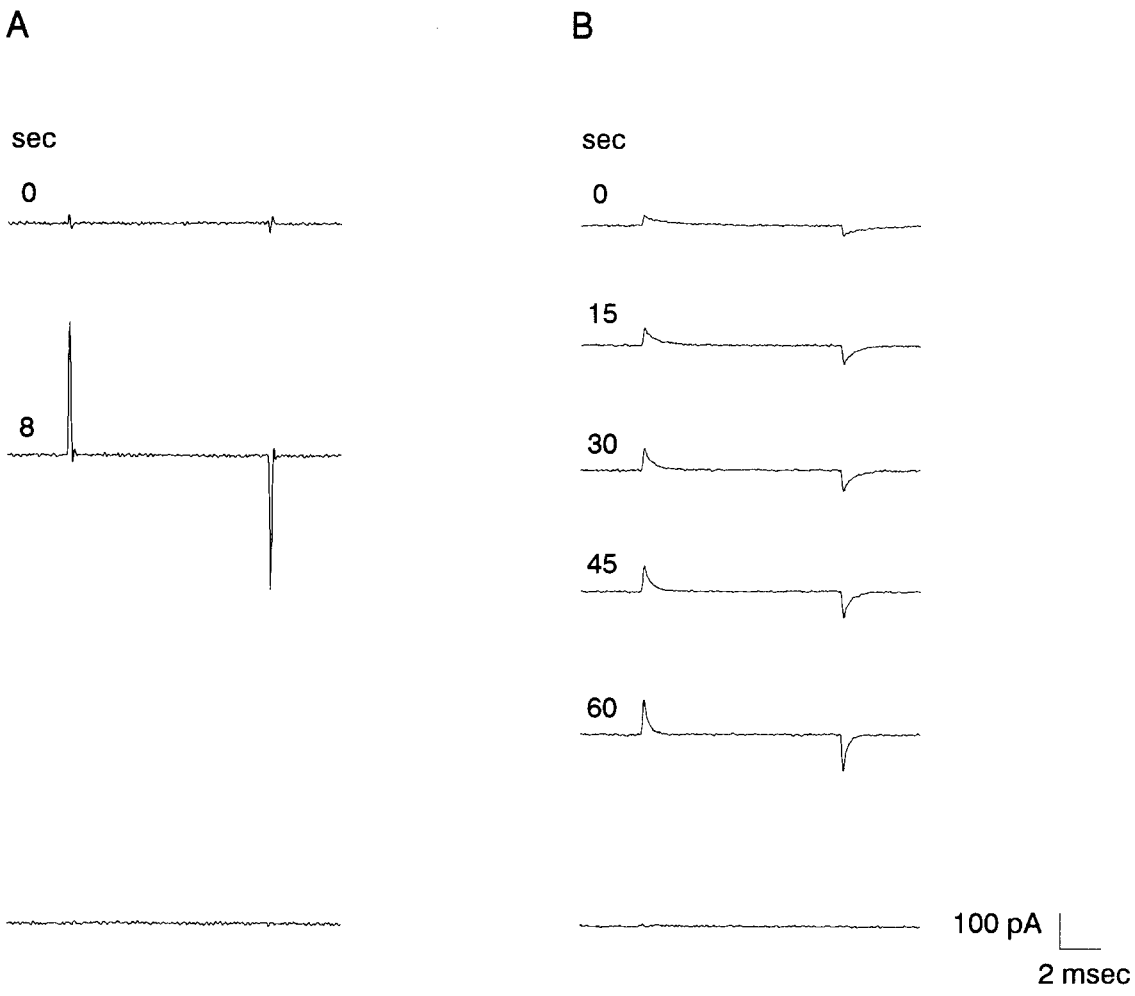

Fig. 1. Capacitive transient cancellation. Pulses (10 mV) from $E = -60$ mV, duration 10 msec, were delivered every 100 msec. T cell current responses were filtered at 5 kHz and sampled every 10 μsec. At time = 0, the C-fast circuitry of the patch-clamp amplifier had already been adjusted to cancel the capacitance of the patch pipette. (*A*) Representative traces during formation of whole-cell configuration. At time = 8 sec the membrane within the electrode was ruptured by applying suction. Final trace was recorded following capacitive cancellation with the C-slow and G-series circuitry of the List amplifier, $C_m = 3.62$ pF, $R_a = 6.5$ MΩ. (*B*) Typical current responses with 75 μg/ml nystatin in the electrode over a period of 1 min. After capacitance due to the cell membrane was cancelled, $C_m = 3.85$ pF, $R_a = 52.6$ MΩ, the bottom trace was recorded.

sient from ~40 μsec (whole-cell) to ~160 μsec (perforated-patch). The cells diminished in size over the course of the experiment, which lasted 25–30 min, in both whole-cell and perforated-patch configuration. In an attempt to correct this situation, the ratio of K-aspartate/KCl was varied in the patch pipette. No ratio (or anion) was found that fully prevents cell shrinkage or swelling (swelling occurs with 140 mM Cl in the pipette). The present solution is a compromise designed to minimize cell volume changes and offset potentials between the patch pipette and bath electrodes. C_m fell in the present report during whole-cell experiments from 4.29 ± 0.34 to 3.63 ± 0.31 pF, and during perforated-patch recordings from 4.68 ± 0.21 to 3.72 ± 0.24 pF. Voltage-gated K^+ channels, as initially proposed by Deutsch and colleagues [8], appear to mediate what is known as regulatory volume decrease (RVD) in response to osmotic shock in peripheral blood lymphocytes [11]. This biological function of T cell K^+ channels may explain why, in our hands, volume loss during patch-clamp experiments was unavoidable. R_a was relatively stable in whole-cell configuration, rising from 9.0 ± 0.8 to 13.3 ± 1.9 MΩ. To evaluate the effects of R_a in perforated-patch configuration, we arbitrarily divided the cells into two groups. In the first group, which is designated high R_a, the series resistance fell from 47.0 ± 2.0 to 37.8 ± 2.8 MΩ; and in the second group, which is termed low R_a, the series resistance fell from 29.1 ± 2.2 to 23.4 ± 2.0 MΩ. The average diameter of the cells was 11.3 μM, assuming 1 μF/cm^2 and a membrane capacitance of 4.0 pF.

Results

Resting Membrane Potential

Immediately after attaining acceptable whole-cell or perforated-patch conditions, the resting membrane

potential (V_m) was recorded for 30–60 sec with the current-clamp circuitry of the List. V_m measurements clustered in two groups: −32 to −45 mV, and −60 to −72 mV. The majority of V_m measurements fell into the first group (33/46) irrespective of recording configuration. The average value of V_m also did not differ significantly between the two techniques (whole-cell: $V_m = -44.5 \pm 2.8$ mV, $n = 19$; perforated-patch: $V_m = -39.7 \pm 2.4$ mV, $n = 27$).

Early Changes in T Cell K^+ Conductance

Voltage-step protocol sequences were aimed at investigating alterations in gK following dissolution of cell membrane integrity, and avoiding "rundown" as long as possible. The first series of voltage steps were begun 1–2 min into recording and were comprised of four depolarizing one-second pulses to 40 mV, delivered every 30 sec. These initial pulses were designed to monitor peak current responses and acceleration in the rate of K^+ current activation and inactivation commonly seen in T lymphocytes during the first 10 min of whole-cell recording [3, 8]. Voltage-step protocols which produced the current responses depicted in Fig. 2 were begun next, 4–5 min after gaining adequate conductivity. When R_a = 35–50 MΩ, the kinetics of activation and inactivation were markedly slower using the perforated-patch technique (Fig. 2). In contrast, as R_a approached 25 MΩ in perforated patches, the fast component of inactivation increased to a point beyond that of whole cell (Fig. 3*C*, Table 1). After waiting 15 min for nystatin pores to form, inactivation rates were typically about 2× faster (Fig. 4), suggesting that the acceleration in inactivation is influenced by the movement of monovalent ions and/or small molecules (less than 200 D) through nystatin pores. In addition, pulses to 40 mV revealed a slight rise in peak currents from 832 ± 70 to 951 ± 49 pA ($n = 9$), during the first 10 min of perforated-patch recordings with high R_a values (35–50 MΩ), and a drop in current maximum from 1,551 ± 215 to 1,208 ± 169 pA ($n = 5$) at low R_a values (R_a = 20–35 MΩ). Peak currents also declined in whole-cell configuration over the same time period from an initial value of 1,462 ± 144 to 1,174 ± 115 pA ($n = 9$).

I-V Relation and Activation Kinetics

Maximum K^+ conductance did not vary significantly between the two methods at 10.4 ± 1.0 nS ($n = 9$) in whole-cell and 10.0 ± 0.8 nS ($n = 14$) in perforated patch. However, maximum gK was reached at very different potentials, 10 mV in standard whole-cell recordings, as opposed to 50 mV under all perforated-patch conditions (Fig. 5*I*). Activation kinetics were taken from the same voltage-step series used to determine K^+ conductance and measured by the amount of time taken to reach current maxima from the beginning of each voltage step. Perforated-patch currents with high R_a values reached a peak at a consistently slower rate, while whole-cell and low R_a perforated-patch experiments had similar if not identical activation kinetics at 0 mV and above (Fig. 5*II*).

Accumulation of Inactivation

K^+ current inactivation not only becomes faster over time during whole-cell recordings, but it is also more complete [3]. To explore this phenomena, a train of voltage steps to 40 mV with a pulse interval of 1 sec, pulse duration 200 msec, was applied to each cell 14–15 min after electrical access was achieved. Peak currents elicited by the second pulse fell by an average of 52% in whole-cell conformation, as compared to 34% in perforated-patch configuration with low R_a, and 21% in perforated patch with high R_a (Fig. 5*III*).

Steady-State Inactivation

Examination of T cell K^+ channel inactivation in relation to the holding potential was accomplished with a standard steady-state inactivation protocol begun 15–16 min into recording. Test pulses to 40 mV were applied every 30 sec from holding potentials of −100 to 0 mV. Steady-state inactivation was shifted in the depolarizing direction by approximately 10 to 20 mV in perforated-patch experiments with both high and low R_a values (Fig. 5*IV*).

Deactivation Kinetics

Tail current protocols were begun after completion of steady-state protocols whenever possible. The seal was lost after holding at 0 mV during steady-state protocols in 3/9 whole-cell experiments and 1/14 perforated-patch experiments. Currents reversed at −78.7 ± 0.5 mV in whole-cell configuration as opposed to −70.4 ± 2.2 mV in perforated patch with high R_a and −70.9 ± 1.3 mV with low R_a. K^+ channel closing was notably different between the two techniques (Fig. 6). Deactivation time constants were 189.3 ± 14.2 msec at −30 mV and 40.9 ± 4.3 msec at −50 mV during whole-cell experi-

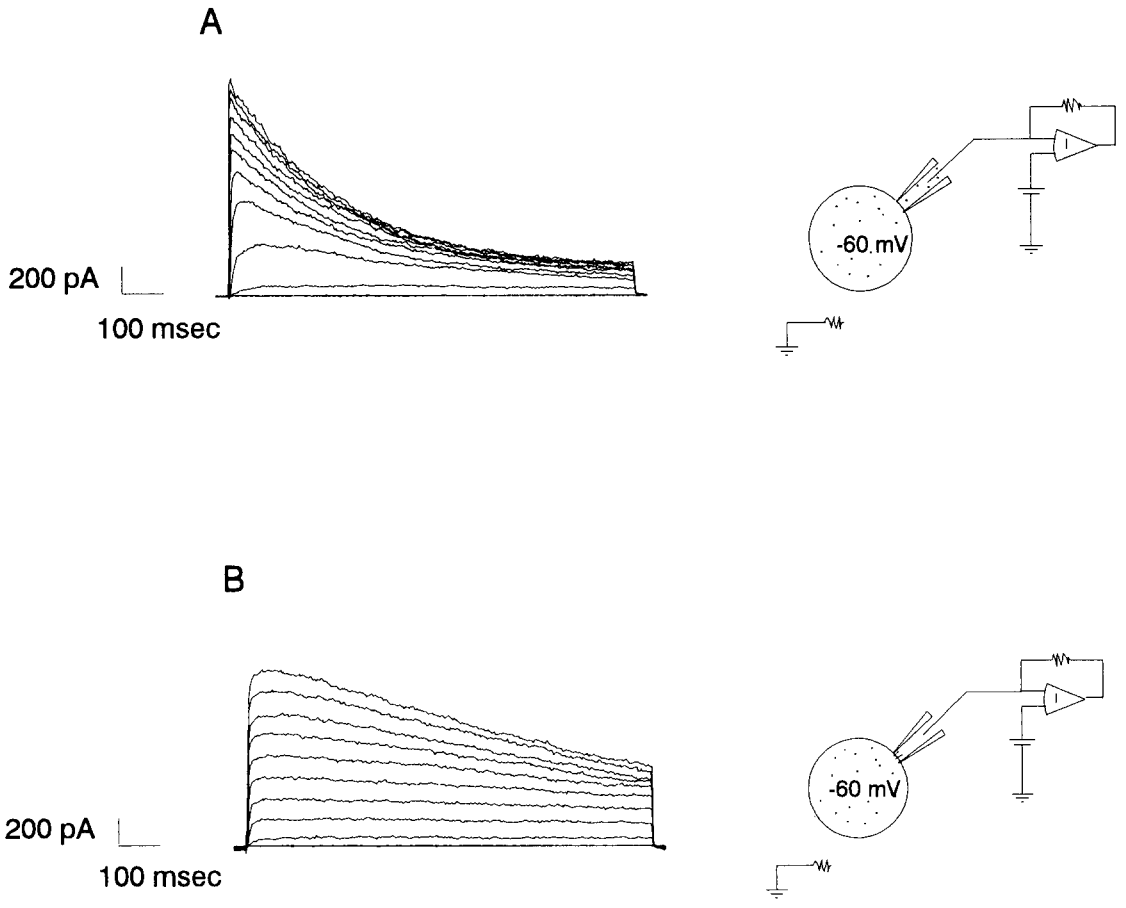

Fig. 2. Whole-cell currents in T cells. Voltage-steps were applied in 10 mV increments for 1 sec from −100 to 60 mV every 30 sec. Sample intervals were 1 msec. (*A*) Whole-cell recording, C_m = 4.13 pF, R_a = 7.9 MΩ. (*B*) Perforated-patch recording, C_m = 4.42 pF, R_a = 50.0 MΩ.

ments as compared to 21.1 ± 4.2 msec and 12.9 ± 2.6, respectively, during perforated-patch experiments with high R_a (42.1 ± 3.7 MΩ). At R_a = 22.6 ± 1.6 MΩ in perforated-patch configuration, deactivation time constants were 22.9 ± 3.2 msec at −30 mV and 9.8 ± 1.2 msec at −50 mV. Time constants were calculated with single exponential functions from currents initially stepped to −10 mV.

Threshold Potentials

The voltage associated with K^+ channel opening or threshold potential in T cells usually shifts −10 to −15 mV during the first 10 min of whole-cell recording, settling around −40 mV [3, 8, 30]. Although early shifts in the voltage dependence of K^+ channel opening were not investigated in the present report, differences in threshold potentials between the two techniques may be related to this phenomenon. Threshold potentials (measured at 5–6 min) averaged −39.4 ± 0.8 mV in whole-cell configuration as opposed to −33.9 ± 0.3 mV (regardless of R_a) in perforated-patch experiments. The voltage at which K^+ channels opened was determined from current maxima by linear regression from voltage steps of −40 to 10 mV during the series of voltage steps shown in Fig. 2.

Recovery from Inactivation

Inactivation recovery was determined 5 min into recording using additional cells. K^+ channels recovered slightly faster from inactivation under perforated-patch conditions as compared to whole cell (Fig. 7).

Ca^{2+}-Free Bath Experiments

Inactivation time constants decreased over time in standard bath solutions in all perforated-patch and whole-cell experiments. To test the hypothesis that

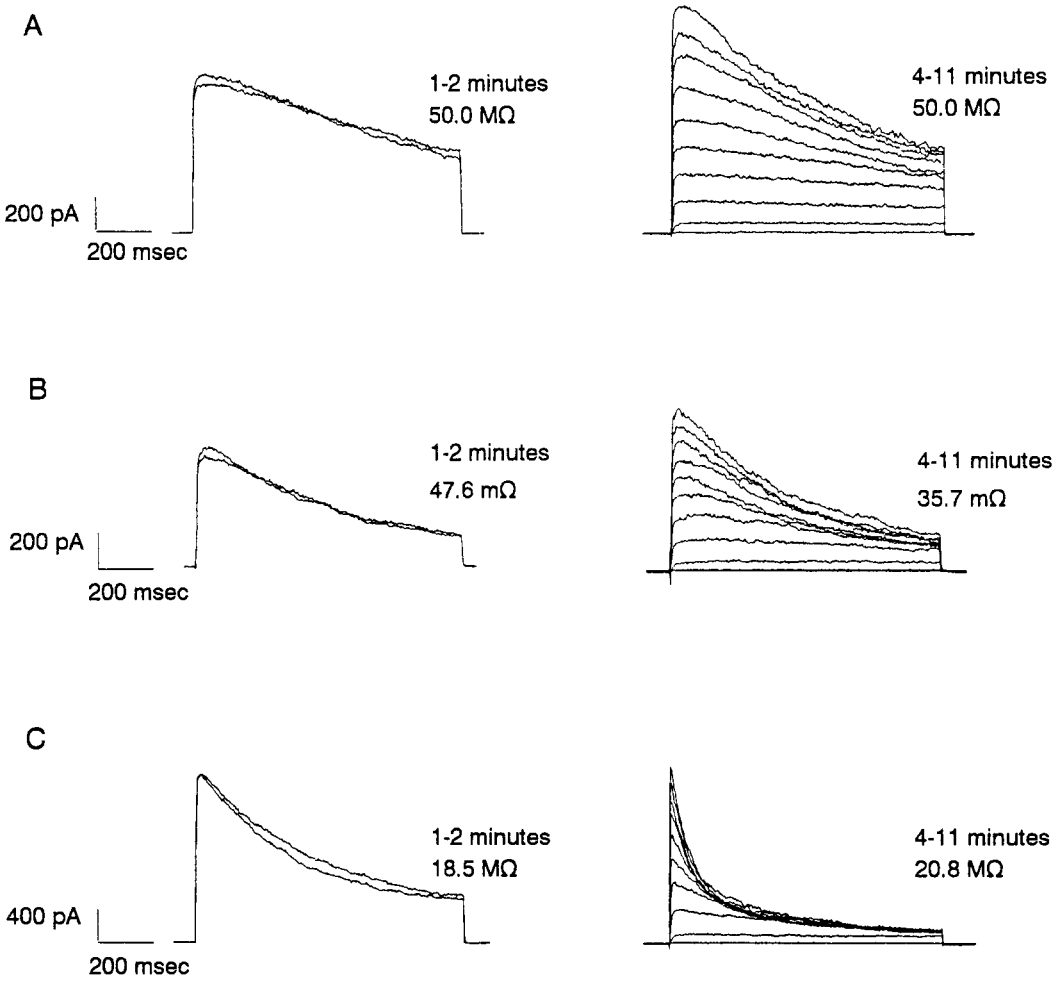

Fig. 3. Perforated-patch inactivation kinetics and their relationship to R_a. T cells were initially challenged with four 100-mV depolarizing voltage steps, delivered every 30 sec. Current responses to the first two pulses are depicted; the second pulse is slightly faster in each case. Next, a voltage-step series was begun 4–5 min after achieving adequate conductivity; pulses were applied in 10-mV increments for 1 sec from −100 to 60 mV every 30 sec (same as in Fig. 2). (*A*) Representative experiment with a stable R_a of 50 MΩ, the peak current of the second pulse is higher, rising from an initial value of 921 to 983 pA. During the voltage-step series shown on the right, the maximum current response to the same voltage challenge was 1,112 pA. (*B*) Typical currents representing the average fall in series resistance during high R_a experiments. Current maxima rose from 581 to 631 pA during the first two pulses, and reached 704 pA during the voltage-step series, approximately 8–9 min later. (*C*) Representative experiment with a relatively stable R_a of ~20 MΩ. The first two current maxima are identical at 2,055 pA; during the voltage-step series, the peak current at 40 mV fell to 1,729 pA.

this increase in inactivation rates may be due to Ca^{2+} ions entering the channel from the outside [12], we challenged T cells with identical voltage protocols in a Ca^{2+}-free bath solution. The increase in the rate of K^+ channel inactivation was left largely unchanged in whole-cell experiments during the first 10 min (Table 2). In contrast, inactivation of the majority of the current was slowed dramatically in Ca^{2+}-free bath solutions in perforated-patch experiments with both high and low R_a values (Table 2). The peak current response behaved virtually the same during whole-cell recordings in Ca^{2+}-free solutions, declining from 1,632 ± 220 to 1,308 ± 177 pA (n = 5). Current maxima remained at approximately the same level during perforated-patch experiments with low R_a, moving from 1,190 ± 199 to 1,167 ± 265 pA (n = 3), and fell in perforated-patch experiments with high R_a values from 1,251 ± 214 to 914 ± 64 pA (n = 5).

The conductance-voltage relationship did not change significantly using either technique in Ca^{2+}-free solutions (Fig. 8). Maximum gK and threshold potentials were also unaltered in Ca^{2+}-free bath solutions [whole cell: maximum gK = 11.5 ± 1.5 nS,

Table 1. Inactivation time constants in standard bath solution

Experimental condition	Minutes into recording	τ_1	I_1	τ_2	I_2
Whole cell[a]					
	1–2	317 ± 52	1,143 ± 130	2,106 ± 485	332 ± 63
	8–9	228 ± 23	959 ± 116	1,379 ± 134	175 ± 43
Perforated patch (high R_a)[b]					
	1–2	931 ± 106	898 ± 65	840 ± 298	131 ± 36
	8–9	686 ± 93	959 ± 78	778 ± 207	144 ± 52
Perforated patch (low R_a)[c]					
	1–2	223 ± 50	828 ± 132	3,578 ± 1,507	355 ± 78
	8–9	120 ± 20	685 ± 79	2,799 ± 1,593	248 ± 62

Time constants were calculated from the current response to the first 100-mV depolarizing pulse applied after acceptable recording conditions were achieved, and the 100-mV pulse delivered 8–9 min later during the series of voltage steps depicted in Fig. 2. Data are represented as the mean ± SEM. τ (msec), I (pA).
[a] $n = 9$, $R_a = 7.9 \pm 0.8$ (begin) to 16.1 ± 2.5 MΩ (end).
[b] $n = 9$, $R_a = 48.9 \pm 1.7$ (begin) to 42.1 ± 3.7 MΩ (end).
[c] $n = 5$, $R_a = 28.4 \pm 3.4$ (begin) to 22.6 ± 1.6 MΩ (end). Currents were fit to a double exponential function as follows:

$$I(t) = I_1 e^{-t/\tau_1} + I_2 e^{-t/\tau_2}$$

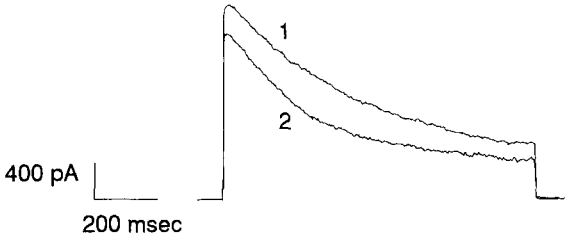

Fig. 4. Alterations in perforated-patch inactivation rates over time. Current responses to the first 100-mV depolarizing pulse, sampled every msec. Time constants were calculated with a double exponential function. (*1*) Representative cell in which nystatin pores formed within the first 2 min, $T_1 = 434$ msec; $T_2 = 9{,}560$ msec, $C_m = 5.56$ pF, $R_a = 18.5$ MΩ (same as in Fig. 3*C*). (*2*) Typical current after waiting 15–20 min for nystatin pores to form, $T_1 = 245$ msec; $T_2 = 5{,}087$ msec, $C_m = 5.14$ pF, $R_a = 35.7$ MΩ.

$E_{open} = -40.4 \pm 0.7$ mV, $n = 5$; perforated patch (regardless of R_a): maximum gK = 9.9 ± 1.2 nS, $E_{open} = -34.6 \pm 0.2$ mV, $n = 8$].

K^+ currents reversed at very similar voltages during Ca^{2+}-free bath experiments [whole cell: -76.1 ± 0.9 mV, $n = 5$; perforated patch: -70.8 ± 1.1 mV, $n = 8$]. However, K^+ channels appeared to close more slowly in a Ca^{2+}-free bath with time constants of 228.9 ± 17.3 msec ($E = -30$ mV) and 49.5 ± 1.6 ($E = -50$ mV) under whole-cell conditions and 53.5 ± 7.9 msec ($E = -30$ mV) and 22.0 ± 1.9 ($E = -50$ mV) in perforated-patch experiments (regardless of R_a).

Discussion

The recording configuration directly affects the kinetics of T cell K^+ currents. Moreover, these kinetic changes cannot be entirely attributed to variations in R_a or liquid junction potentials. Inactivation increases over time in all whole-cell and perforated-patch configurations. After approximately 10 min, inactivation is fastest in perforated-patch recordings with low R_a values (20–33 MΩ), and it is slowest during perforated-patch experiments with relatively high R_a values (35–50 MΩ). By comparison, during the same time period, inactivation appears to stabilize at an intermediate level in whole-cell configuration (R_a = 5–12 MΩ). In contrast, deactivation kinetics are essentially identical in all perforated-patch experiments, regardless of R_a, and are slowest in whole-cell configuration. R_a discrepancies introduce an error in the *I-V* relationship, and may slow the rate at which currents activate and inactivate in high R_a experiments by shifting the voltage curve to the right. However, differences in R_a values or junction potentials cannot explain the increase in inactivation during low R_a experiments or the ubiquitous increase in channel closing during all perforated-patch experiments.

Whole-cell K^+ conductance reaches a maximum at potentials approximately 40 mV more negative than perforated-patch K^+ conductance. Threshold potentials as well as reversal potentials were also shifted in a negative direction during whole-cell recordings but to a lesser extent (5 to 8 mV, respec-

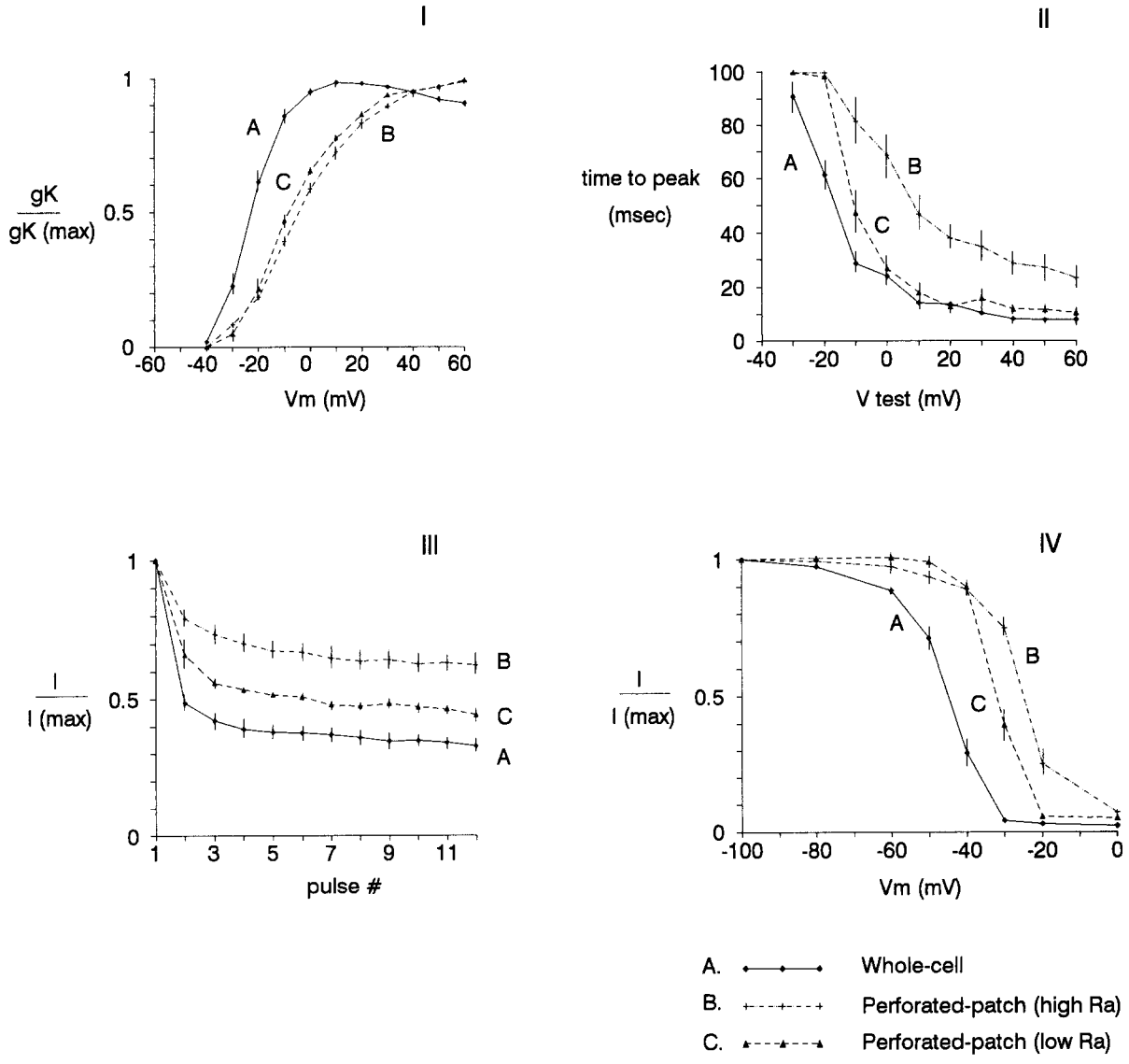

Fig. 5. Normalized data comparing the conductance-voltage relation, activation kinetics, cumulative inactivation, and steady-state inactivation during whole-cell and perforated-patch recordings. Data are represented as mean ± SEM. (*A*) Whole cell (n = 9), R_a rose from 7.9 ± 0.8 to 16.1 ± 2.5 MΩ. (*B*) Perforated-patch (n = 9), R_a fell from 48.9 ± 1.6 to 42.1 ± 3.7 MΩ. (*C*) Perforated-patch (n = 5), R_a fell from 28.4 ± 3.4 to 22.6 ± 1.6 MΩ. (*I*) Conductance-voltage relation. Current responses were taken from the voltage-step series begun 4–5 min after attaining electrical access to the cells (same as in Figs. 2 and 3). Potassium conductance (gK) was calculated by the formula:

$$gK = I(peak)/(V - E_{rev})$$

E_{rev} was determined individually using the instantaneous *I-V* relation, when available, or assumed to be −78.7 mV during whole-cell recordings and −70.6 mV during perforated-patch experiments. (*II*) Activation kinetics as measured by the time to peak current. Current responses were taken from the same voltage-step series as in Fig. 4*I* sampled every 100 μsec. A number of currents reached a sustained plateau during voltage steps from −30 to −10 mV and were assigned a time to peak of 100 msec to facilitate graphic representation. (*III*) Cumulative inactivation. Voltage steps of 100 mV, duration 200 msec, sample interval 20 μsec, were delivered every second approximately 14–15 min into recording. Data were normalized by assigning *I* (max) to the peak current of the first pulse. (*IV*) Steady-state inactivation. Holding potentials of E = −100 mV to E = 0 mV were maintained for 30 sec prior to challenging the membrane with a 1-sec pulse to 40 mV. Data were normalized by assigning *I* (max) to the peak current of the first pulse.

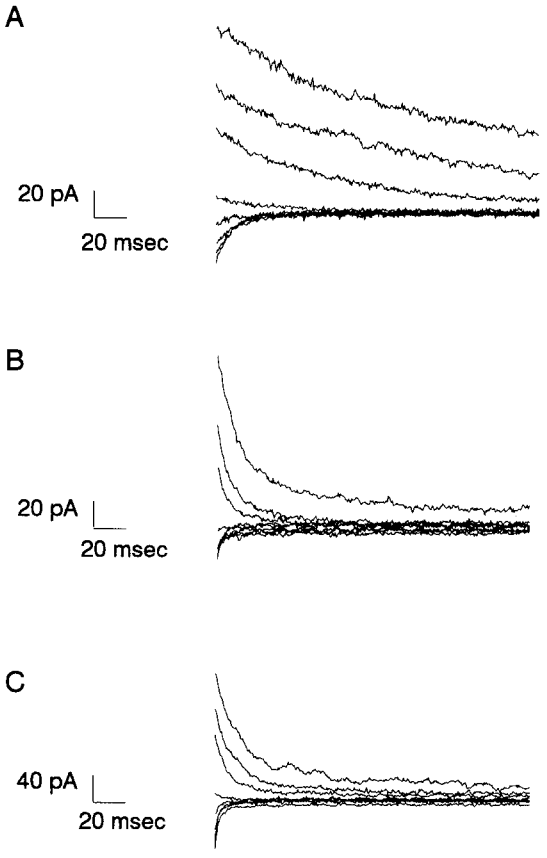

Fig. 6. Instantaneous current-voltage (*I-V*) relation. T cells were depolarized to −10 mV for 100 msec then stepped to voltages ranging from −30 to −110 mV for an additional 200 msec before returning to the holding potential (E = −60 mV). Pulses were applied every 30 sec. Representative currents from T cells in whole-cell and perforated-patch configurations were sampled every 200 μsec. (*A*) Whole cell, C_m = 4.13 pF, R_a = 7.9 MΩ. (*B*) Perforated patch, C_m = 3.26 pF, R_a = 50.0 MΩ. (*C*) Perforated patch, C_m = 4.45 pF, R_a = 20.8 MΩ.

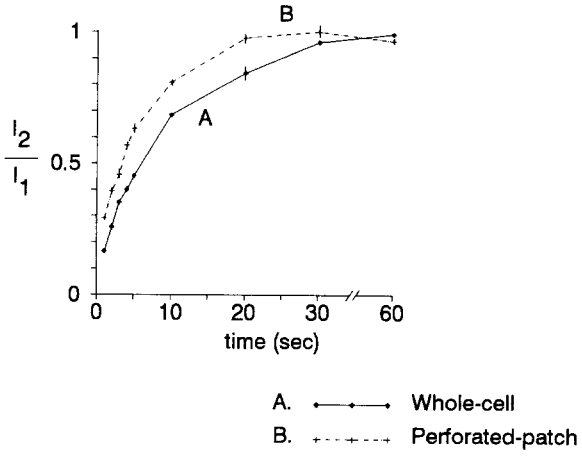

Fig. 7. Recovery from inactivation. Twin pulses to 40 mV were applied every 90 sec. Pulse length was 500 msec, time between pulses ranged from 1 sec to 60 sec and is represented on the abscissa. Data were normalized by assigning I_1 to the current maxima of the first pulse minus its minimum, and I_2 to the current maxima of the second pulse minus the minimum value of the first. Mean ± SEM. (*A*) Whole cell (n = 5), R_a = 8.0 ± 0.9 (begin) to 10.5 ± 2.4 MΩ (end). (*B*) Perforated patch (n = 5), R_a = 47.3 ± 2.8 (begin) to 27.0 ± 2.3 MΩ (end).

tively). Differences in R_a values and liquid junction potentials probably contribute to these disparities but cannot account for them entirely. If, for example, a large chloride disequilibrium existed across perforated patches, V_m measurements might be lowered as much as −57.5 mV (assuming internal chloride = 3 mM, and perfect chloride selectivity). However, junction potential differences between whole-cell and perforated-patch configuration were, in effect, measured in current clamp mode by holding I = 0, and V_m measurements differed between the two techniques by only an average of 4.8 mV. If R_a represents only the resistance between the cytosol and patch pipette, the potential drop across perforated patches would be equal to 50 mV, when I_K = 1 nA, R_a = 50 MΩ; and 25 mV, when I_K = 1 nA, R_a = 25 MΩ. However, R_a measurements actually include resistances of the electrode, patch, cell, and seal. Since maximal gK was reached at nearly identical potentials in all perforated-patch experiments independently of R_a, the resistance of the cell, or the channels in its membrane, must also contribute to the difference in the conductance-voltage relationship.

T cell K^+ channel inactivation is enhanced by increasing either internal or external Ca^{2+} concentrations, and decreased by raising K^+ concentrations, suggesting competition between K^+ and Ca^{2+} for the same site within the channel [2, 12]. Perforated-patch experiments revealed the expected relationship between external Ca^{2+} ion levels and inactivation, while whole-cell inactivation rates decayed in a surprisingly similar manner in both standard and Ca^{2+}-free bath solutions. In the present report, whole-cell internal solutions contained Ca^{2+} ion concentrations of 10^{-7} M, which may have masked the influence of external Ca^{2+}. As a precedent for this, after varying Ca^{2+} concentrations on both the inside and outside of the T cell line, Jurkat, Grissmer and Calahan [12] reported that internal Ca^{2+} levels influenced the effect of external Ca^{2+} on K^+ current inactivation rates.

Whole-cell peak current amplitudes fell approximately 20% in both standard and Ca^{2+}-free bath solutions. A voltage shift is probably not involved, because the negative shift in the *I-V* relation which ordinarily occurs during the first 10 min of whole-cell recording would raise peak currents, not lower

Table 2. Inactivation time constants in Ca-free bath solution

Experimental condition	Minutes into recording	τ_1	I_1	τ_2	I_2
Whole cell[a]					
	1–2	264 ± 16	1,090 ± 140	2,463 ± 913	429 ± 87
	8–9	230 ± 20	923 ± 144	1,456 ± 287	363 ± 125
Perforated patch (high R_a)[b]	1–2	1,263 ± 188	1,192 ± 151	1,149 ± 349	136 ± 79
	8–9	1,623 ± 356	918 ± 63	974 ± 328	75 ± 31
Perforated patch (low R_a)[c]					
	1–2	1,322 ± 384	960 ± 174	246 ± 33	219 ± 107
	8–9	758 ± 231	608 ± 148	718 ± 537	205 ± 119

Time constants were calculated as in Table 1. Data are represented as the mean ± SEM. τ (msec), I (pA).
[a] $n = 5$, $R_a = 9.4 \pm 1.3$ (begin) to 14.4 ± 4.6 MΩ (end).
[b] $n = 5$, $R_a = 37.4 \pm 7.3$ (begin) to 43.8 ± 2.9 MΩ (end).
[c] $n = 3$, $R_a = 30.2 \pm 1.6$ (begin) to 24.8 ± 4.5 MΩ (end).

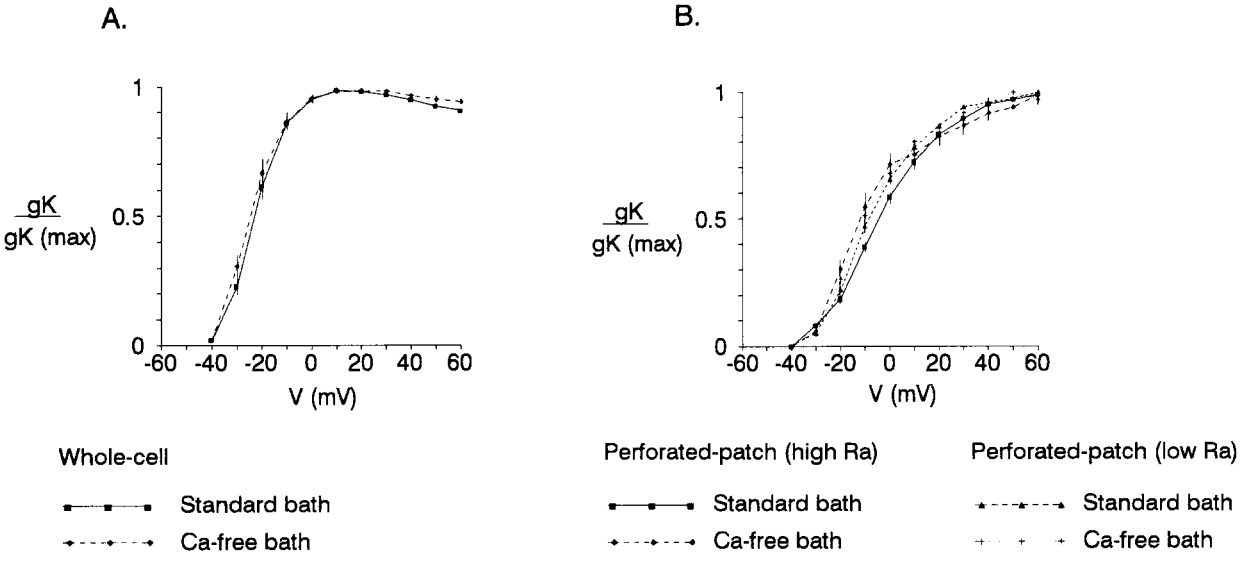

Fig. 8. Potassium conductance (gK) in standard bath (same as in Fig. 4) and Ca-free bath solutions. Mean ± SEM. (*A*) Whole-cell configuration: Standard bath ($n = 9$), $R_a = 7.9 \pm 0.6$ (begin) to 16.1 ± 2.5 MΩ (end); Ca-free bath ($n = 5$), $R_a = 9.4 \pm 1.4$ (begin) to 14.4 ± 2.9 MΩ (end). (*B*) Perforated-patch configuration: High R_a/standard bath ($n = 9$), $R_a = 48.9 \pm 1.6$ (begin) to 42.1 ± 3.7 MΩ (end); High R_a/Ca-free bath ($n = 5$), $R_a = 41.7 \pm 4.6$ (begin) to 43.6 ± 2.9 MΩ (end); Low R_a/standard bath ($n = 5$), $R_a = 28.4 \pm 3.4$ (begin) to 22.6 ± 1.6 MΩ (end); Low R_a/Ca-free bath ($n = 3$), $R_a = 30.2 \pm 1.6$ (begin) to 24.8 ± 4.5 MΩ (end).

them [3, 8, 30]. The consistent fall in K^+ currents in whole-cell configuration may be due to a use-dependent block of the channels by an internal Ca^{2+} concentration of 10^{-7} M. Although a direct comparison between this report and others is not available, internal Ca^{2+} concentrations of 10^{-6} M have decreased T lymphocyte gK during the first 5 min of whole-cell recording, while internal Ca^{2+} concentrations of 10^{-8} M increased gK over the same time period [2, 3]. Alternatively, the decline in gK may be attributed to the loss of a cellular component which influences the voltage sensitivity of the channel. During steady-state inactivation, at holding potentials of −40 mV, close to the average resting membrane potential of −44.5 mV in whole-cell experiments, only 30% of the current is left, and yet the largest currents are recorded upon first breaking into whole-cell configuration.

In physiologic solutions, current maxima fell by 21% in perforated-patch experiments with low R_a and remained relatively stable in Ca^{2+}-free solutions. The loss of a cytosolic constituent which influences voltage-dependent inactivation is not as likely in this case due to the disparity between bath solutions, and because 99% of the current is still present at holding potentials as low as −50 mV. It

seems more probable that the decay of gK over time in low R_a experiments is due to an altered cytoplasmic ionic environment, created by the diffusion of monovalent ions through nystatin pores, which may influence the extent of divalent ion inactivation and/or block of the channel. In conjunction with this, the increase in the fast component of inactivation during low R_a experiments in perforated-patch configuration is strikingly similar to that found when raising external Ca^{2+} from 2 mM to 12 mM in whole-cell configuration [12]. Comparisons between cells in which nystatin pores formed over a period of 1–2 min as opposed to 15–20 min present further evidence that the movement of monovalent ions (or small neutral molecules) through nystatin pores influences K current kinetics (*see* Fig. 4).

The 12.5% increase in K^+ currents in standard bath solutions during perforated-patch recordings with high R_a could be attributed to a decline in the series resistance, which would shift the *I-V* relation to the left. However, when R_a values remained stable, the currents continued to rise (example in Fig. 3*A*). A removal of voltage-dependent inactivation by holding potentials of −60 mV may have raised currents in this case because 11% of the current is inactivated at holding potentials of −40 mV, which approaches the resting membrane potential. Alternatively, patches with fewer nystatin pores may retard equilibration between the pipette solution and cytosol, particularly of monovalent anions, such as aspartate [14, 18], and allow a use-dependent unblock of the channels by K^+ entry to occur. We favor a use-dependent unblock, because in contrast to the increase in standard bath solutions, current maxima fell by 26.8% in Ca^{2+}-free bath solutions during high R_a recordings. Ca^{2+}-dependent block of the channels has been estimated at approximately 25% under normal conditions, and the loading of blocking Ca^{2+} ions (as opposed to inactivating) appears to occur exclusively from the inside [12]. As first proposed by Grissmer and Calahan [12], Ca^{2+} may be able to leave this blocking site when the channel is closed. Our data support this contention, because Ca^{2+} ions loaded from the inside would be expected to move through the channel to the outside in a Ca^{2+}-free bath solution, increasing K^+ currents by approximately 25% during the initial pulse.

Activation and inactivation rates were slowest during perforated-patch recordings with high R_a. Again, this may simply reflect a shift in the *I-V* curve, or may be related to the diffusion rates of monovalent ions and small molecules through nystatin pores. Both of these events probably contribute to the slower kinetics of high R_a experiments. However, the latter possibility appears to contribute the greater share, because at R_a = 35.7 MΩ, after waiting 15 min for the nystatin pores to form, inactivation time constants are very close to whole-cell values (Fig. 4).

The accumulation of inactivation gradually increases in human T cell K^+ channels following rupture of the membrane or "break-in" during whole-cell recording [3]. The extent of inactivation is not as great at metabolic temperatures and recovery from cumulative inactivation is also markedly faster at 37°C as opposed to 25°C [20]. The onset of accumulation of inactivation in the current report was slower in perforated-patch configuration and was not as complete. Taken together, these results suggest that a temperature-sensitive, biochemical pathway which is influenced by the recording configuration may regulate K^+ channel inactivation. This hypothesis is supported by results from standard recovery protocols. Shaker K^+ channel inactivation analysis, using trypsin digests, deletion mutants, and synthetic peptides, conforms to a cytoplasmic "ball and chain model" of inactivation with both fast and slow components [15, 32]. Due to the close homology between Shaker K^+ channels and T cell K^+ channels it seems reasonable to propose that a metabolic event, such as phosphorylation of an analogous region, may regulate lymphocyte K^+ channel inactivation.

Steady-state inactivation varied in accordance with the recording configuration and, thus appeared to depend on the series resistance. However, holding potentials were virtually equivalent in all experiments because, as the current approaches zero, so does the potential drop between the cytosol and patch pipette. Also, current maxima were normalized, which should eliminate errors due to variations in R_a as the currents rose. At holding potentials of −40 mV, 89% of the current was left in perforated-patch configuration regardless of R_a, as compared to 29% during whole-cell experiments. Discrepancies in steady-state inactivation occurred between whole-cell and perforated-patch experiments from −60 to −30 mV, and within perforated-patch experiments from −30 to −20 mV. Therefore, it appears likely that the voltage-dependent inactivation of T cell K^+ channels is influenced by the loss of a cellular component in whole-cell configuration, as well as by the movement of diffusible elements through nystatin pores.

Tail currents were noticeably slower in whole-cell, as opposed to perforated-patch configuration. Comparable differences in deactivation time constants are seen in murine lymphocyte type *n* (normal) and *l* (lpr) channels [4, 6, 21]. Moreover, differences between perforated-patch and whole-cell currents in the conductance-voltage relation and steady-state inactivation are similar to "*l*" and "*n*" type designa-

tions, respectively. In its homozygous state the *lpr* gene mutation is associated with lymphadenopathy, acceleration of autoimmune phenomena, and constitutive phosphorylation of the TCR-CD3 zeta chain [27]. As previously discussed by DeCoursey et al. [6], the *lpr* gene locus may modulate cellular constituents which regulate lymphocyte K^+ channels. We present evidence in this report that some of these cellular components are conserved in perforated-patch configuration.

In conclusion, by blocking the diffusion of relatively large cellular components into the pipette, and retarding the equilibration of monovalent ions and/or small neutral molecules, the perforated-patch technique appears to have dramatically altered the behavior of K^+ channels in activated human T cells. Although perforated-patch experiments sacrifice the voltage-clamp quality, they appear to provide an additional means of identifying biochemical pathways which regulate T lymphocyte K^+ channel characteristics.

We thank Kathleen Brattain for useful comments on the manuscript. This work was supported by NIDA grants DA04498-03 and DA01451-15, the State of Georgia Human Resources Department, and an Individual National Research Service Award presented to D.R.O. from NIAAA.

References

1. Akbar, A.N., Terry, L., Timms, A., Beverley, P.C.L., Janossy, G. 1988. Loss of CD45R and gain of UCHL1 reactivity is a feature of primed T cells. *J. Immunol.* **140:**2171–2178
2. Bregestovski, P., Redkozubov, A., Alexeev, A. 1986. Elevation of intracellular calcium reduces voltage-dependent potassium conductance in human T cells. *Nature* **319:**776–778
3. Cahalan, M.D., Chandy, K.G., DeCoursey, T.E., Gupta, S. 1985. A voltage-gated potassium channel in human T lymphocytes. *J. Physiol.* **358:**197–237
4. Chandy, K.G., DeCoursey, T.E., Fischback, M., Talal, N., Cahalan, M.D., Gupta, S. 1986. Altered K^+ channel expression in abnormal T lymphocytes from mice with *lpr* gene mutation. *Science* **233:**1197–1199
5. DeCoursey, T.E., Chandy, K.G., Gupta, S., Cahalan, M.D. 1984. Voltage-gated K^+ channels in human T lymphocytes: a role in mitogenesis? *Nature* **307:**465–468
6. DeCoursey, T.E., Chandy, K. G., Gupta, S., Cahalan, M.D. 1987. Two types of potassium channels in murine T lymphocytes. *J. Gen. Physiol.* **89:**379–404
7. Desai, D., Newton, M., Kadlecek, T., Weiss, A. 1990. Stimulation of the phosphatidyl-inositol pathway can induce T-cell activation. *Nature* **348:**66–69
8. Deutsch, C., Krause, D., Lee, S.C. 1986. Voltage-gated potassium conductance in human T lymphocytes stimulated with phorbol ester. *J. Physiol.* **372:**405–423
9. Douglass, J., Osborne, P.B., Cai, Y.C., Wilkinson, M., Christie, M.J., Adelman, J.P. 1990. Characterization and functional expression of a rat genomic DNA clone encoding a lymphocyte potassium channel. *J. Immunol.* **144:**4841–4850
10. Gelfand, E.W., Cheung, R.K., Grinstein, S. 1984. Role of membrane potential in the regulation of lectin-induced calcium uptake. *J. Cell Physiol.* **121:**533–539
11. Grinstein, S., Smith, J.D. 1990. Calcium-independent cell volume regulation in human lymphocytes. *J. Gen. Physiol.* **95:**97–120
12. Grissmer, S., Cahalan, M.D. 1989. Divalent ion trapping inside potassium channels of human T lymphocytes. *J. Gen. Physiol.* **93:**609–630
13. Guy, H.R., Conti, F. 1990. Pursuing the structure and function of voltage-gated channels. *Trends Neurosci.* **13:**201–206
14. Horn, R., Marty, A. 1988. Muscarinic activation of ionic currents measured by a new whole-cell recording method. *J. Gen. Physiol.* **92:**145–159
15. Hoshi, T., Zagotta, W.N., Aldrich, R.W. 1990. Biophysical and molecular mechanisms of Shaker potassium channel inactivation. *Science* **250:**533–538
16. Imboden, J., Weyand, C., Goronzy, J. 1987. Antigen recognition by a human T cell clone leads to increases in inositol trisphosphate. *J. Immunol.* **138:**1322–1324
17. Ishida, Y., Chused, T.M. 1988. Heterogeneity of lymphocyte calcium metabolism is caused by T cell-specific calcium-sensitive potassium channel and sensitivity of the calcium ATPase pump to membrane potential. *J. Exp. Med.* **168:**839–852
18. Korn, S.J., Horn, R. 1989. Influence of sodium-calcium exchange on calcium current rundown and the duration of calcium-dependent chloride currents in pituitary cells, studied with whole cell and perforated patch recording. *J. Gen. Physiol.* **94:**789–812
19. Kvanta, A., Gerwins, P., Jondal, M., Fredholm, B. 1990. Stimulation of T-cells with OKT3 antibodies increases forskolin binding and cyclic AMP accumulation. *Cell. Signal* **2:**461–470
20. Lee, S.C., Deutsch, C. 1990. Temperature dependence of K^+-channel properties in human T lymphocytes. *Biophys. J.* **57:**49–62
21. Lewis, R.S., Cahalan, M.D. 1988. Subset-specific expression of potassium channels in developing murine T lymphocytes. *Science* **239:**771–775
22. Lewis, R.S., Cahalan, M.D. 1989. Mitogen-induced oscillations of cytosolic Ca^{2+} and transmembrane Ca^{2+} current in human leukemic T cells. *Cell. Regul.* **1:**99–112
23. Lindau, M., Fernandez, J. 1986. IgE-mediated degranulation of mast cells does not require opening of ion channels. *Nature* **319:**150–153
24. Matteson, D.R., Deutsch, C. 1984. K channels in T lymphocytes: a patch clamp study using monoclonal antibody adhesion. *Nature* **307:**468–471
25. Mustelin, T., Coggeshall, K.M., Isakov, N., Altman, A. 1990. T cell antigen receptor-mediated activation of phospholipase C requires tyrosine phosphorylation. *Science* **247:**1584–1587
26. Oettgen, H.C., Terhorst, C., Cantley, L.C., Rosoff, P.M. 1985. Stimulation of the T3-T Cell receptor complex induces a membrane-potential-sensitive calcium influx. *Cell* **40:** 583–590
27. Samelson, L.E., Davidson, W.F., Morse, H.C., III, Klausner, R.D. 1986. Abnormal tyrosine phosphorylation on T-cell receptor in lymphoproliferative disorders. *Nature* **324:**674–676
28. Sanders, M.E., Makgoba, M.W., Sharrow, S.O., Stephany, D., Springer, T.A., Young, H.A., Shaw, S. 1988. Human memory T lymphocytes express increased levels of three cell

adhesion molecules (LFA-3, CD2, and LFA-1) and three other molecules (UCHL1, CDw29, and Pgp-1) and have enhanced IFN-gamma production. *J. Immunol.* **140:**1401–1407
29. Sanders, M.E., Makgoba, M.W., Shaw, S. 1988. Human naive and memory T cells: reinterpretation of helper-inducer and suppressor-inducer subsets. *Immunol. Today* **9:**195–199
30. Schlichter, L., Sidell, N., Hagiwara, S. 1986. K channels are expressed early in human T-cell development. *Proc. Natl. Acad. Sci. USA* **83:**5625–5629
31. Vita, A., Pacini, A., Pessina, G.P., Muscettola, M., Paulesu, L., Fanetti, G. 1987. DNA synthesis and interferon release by human peripheral lymphocytes exposed to high potassium medium. *Proc. Soc. Exp. Biol. Med.* **184:**133–137
32. Zagotta, W.N., Hoshi, T., Aldrich, R.W. 1990. Restoration of inactivation in mutants of Shaker potassium channels by a peptide derived from ShB. *Science* **250:**568–571

Received 27 March 1992; revised 27 October 1992